Correlation between a negative group velocity and a slanted stop band in two-dimensionally periodic structures

R. B. Hwang

Department of Communication Engineering, National Chiao Tung University, Hsinchu, Taiwan

Received 28 February 2005; revised 15 July 2005; accepted 7 November 2005; published 10 February 2006.

[1] In this paper, we employed the rigorous mode-matching method to carry out the calculation for the scattering characteristics of a two-dimensionally periodic structure made up of metallic rectangular cylinders. From the scattering characteristics, the interesting phenomenon of an anomalous dispersion was observed to possess negative group velocities. In order to understand the underlying physics involved, we begin with the investigation of the band structure associated with the corresponding structure of infinite extent; thereby, the band structures are classified into two types: vertical stop band that is mainly due to the effect of periodicity in a single direction and slanted stop band that is due to the combined effects of periodicities in two directions. Notably, the negative group velocity (delay) within the slanted stop band of a two-dimensional periodic structure was directly related to the experimentally measurable scattering characteristics of the finite structure.

Citation: Hwang, R. B. (2006), Correlation between a negative group velocity and a slanted stop band in two-dimensionally periodic structures, *Radio Sci.*, *41*, RS1004, doi:10.1029/2005RS003262.

1. Introduction

[2] The class of periodic structures has been a subject of continuing interest in the literature. The main effort in the past had been on the scattering and guiding of waves by one-dimensionally periodic structures [*Rotman*, 1951; *Elliott*, 1954]. Recently, considerable attention has been focused on the study of wave phenomena associated with two-dimensional (2-D) ones, particularly in conjunction with the properties of photonic band gap [*Fan et al.*, 1996; *Sigalas et al.*, 1995]. Since wave propagation is forbidden in the stop band, this allows us to mold the power flow or to inhibit spontaneous emission. Consequently, many novel dielectric (optical) waveguides or cavities were developed by using the photonic band gap material. For example, the waveguide with 2-D periodic structures as its walls was designed to make the waves bounce back and forth around the channel [*Mekis et al.*, 1999; *Hwang and Peng*, 2003].

[3] In addition to the properties of strong reflection in the stop band, the anomalous refraction, such as ultra-refraction (or negative refraction), was found to exist in such a class of 2-D periodic structures, especially in the vicinity of the band edge [*Enoch et al.*, 2003; *Boris et al.*, 2000; *Notomi*, 2000]. Many researchers took advantage of these properties to design lenses with a very short focal length or to confine emission in a narrow lobe [*Gralak et al.*, 2000; *Boris et al.*, 2000]. It is noted that the previous research works were made under the condition that the spatial periods of the photonic band gap materials are of the order of operation wavelength.

[4] In addition to the behavior of wave reflection in stop band associated with a photonic band gap structure, the negative and infinite group velocities were experimentally observed in bulk hexagonal two-dimensional photonic band gap crystals within the band gap in the microwave region [*Solli et al.*, 2003]. On the basis of their experimental studies, they found that the crystal exhibits anomalous dispersion within the band gap, passing through zero dispersion at the band edges. In addition, the negative phase and group velocities, along with positive group and negative phase velocities (i.e., backward waves), were theoretically investigated by using a simple model to characterize the property of negative refractive index (NRI) of a metamaterial [*Mojahedi et al.*, 2003]. Recently, the same group had extended the work to design a medium which not only possesses NRI properties but also exhibits negative

0048-6604/06/2005RS003262

group velocities (NGV). In their invention, a resonant circuit is embedded within each loaded transmission line unit cell, resulting in a region of anomalous dispersion for which the group delay is negative [*Siddiqui et al.*, 2003].

[5] In a recent publication [*Hwang*, 2004], we have investigated the relationship between the scattering characteristic and the band structure of a two-dimensionally electromagnetic crystal containing a metal and dielectric medium. Therein, we have demonstrated the relationship between the transmission spectrum and the band structure of a 2-D periodic structure. Specifically, two types of stop band were clearly identified: one is referred to as the vertical type and the other as the slanted type. The former consists of the commonly known stop bands that are due to the effect of one-dimensional periodicity; thus each vertical stop band has a constant phase over the entire stop band. On the other hand, the later consists of the stop bands that are slanted at an angle on the k_o-β diagram (a part of the standard Brillouin diagram) and that are attributed to the combined effect of the periodicities in two dimensions. Notably, the 1-D periodic structure can also support the slanted stop band. The dispersion analysis of the shielded Sievenpiper structure [*Elek and Eleftheriades*, 2004] has been proved to support the slanted stop band, caused by the contradirectional coupling between the fundamental backward-wave harmonic and an underlying forward parallel-plate mode.

[6] In this paper, we present a thorough investigation of a 2-D periodic structure that is composed of rectangular metallic cylinders immersed in a uniform medium. Since the shape of the metallic cylinders considered here is rectangular and the material is assumed to be a perfect electric conductor, the electric fields inside the metal cylinder are zero, and those outside the metal region are expressed in terms of the superposition of waveguide modes (parallel-plate waveguide modes). These waveguide modes inherently satisfy the electromagnetic boundary condition; therefore this could speed up the numerical convergence for the tangential electric and magnetic fields. Besides, in the numerical computation, all the mathematical procedures resort to the matrix operation; the dimensions of these matrices are proportional to the number of space harmonics (waveguide modes) truncated. Thus the speed of computation and required memory space directly relate to the number of space harmonics. To ensure the accuracy of numerical results, we have carried out convergence tests for both the scattering and dispersion analyses against the number of space harmonics (or waveguide modes). We found that a small number of space harmonics is needed to achieve the power conservation criterion.

[7] The mode-matching method utilized in this paper could have the advantages as described previously. However, for the metallic cylinders with curved profile, such as circular ones, the present method remains to be improved. Although the staircase approximation could be used to partition the curved profile into a stack of rectangular layers, this would make the mathematical formulation complicated, and the artificial edges caused by the piecewise approximation would result in extra edge diffraction (especially in higher-frequency operation). The method of Green's function based on lattice sums is more suitable for such type of problems [*Botten et al.*, 2000].

[8] Concerning the mathematical procedures for this research work, first, the scattering of a plane wave by a structure of finite thickness was analyzed with particular attention directed to the variation of the group velocity (index) in terms of the phase angle of the transmittance spectrum. Then, we calculated the dispersion characteristics of a structure of infinite extent, including the phase constant (real part) and attenuation constant (imaginary part), as plotted in the form of the k_o-β diagram. By comparison between the scattering and dispersion characteristics, we have observed the negative group delay to exist in the region of slanted stop bands but not in the vertical ones.

[9] This paper is organized as follows. In section 2, we first introduce the structure configuration and incident conditions for the 2-D periodic structure under consideration. In section 3, we outline the mathematical formulations to resolve such a 2-D boundary value problem. The method of mode matching and the Floquet solutions were employed to transform the electromagnetic field problem into a representation of transmission line network. Moreover, the generalized scattering matrix representation and the Bloch condition were utilized to obtain a generalized eigenvalue problem for determining the dispersion relation of waves propagating in such an infinite 2-D periodic medium. The scattering characteristics, including the reflectance and transmittance of each space harmonic, were also calculated. In section 4, we carried out numerous numerical calculations on the group delay via the transmittance of plane wave at an oblique incidence. Moreover, the dispersion relation of a 2-D periodic medium was calculated and was demonstrated to verify the negative group velocity in the slanted stop band region. In section 5, we conclude this paper by making some remarks.

2. Description of the Problem

[10] The structure under consideration is a 2-D periodic structure with finite thickness. As shown in Figure 1a, the rectangular metal rods are immersed in a dielectric host medium. The array of rods repeats itself infinitely in the x direction but is finite in the y direction. Such a structure is assumed to be uniform along the z direction and can be regarded as a finite stack of 1-D

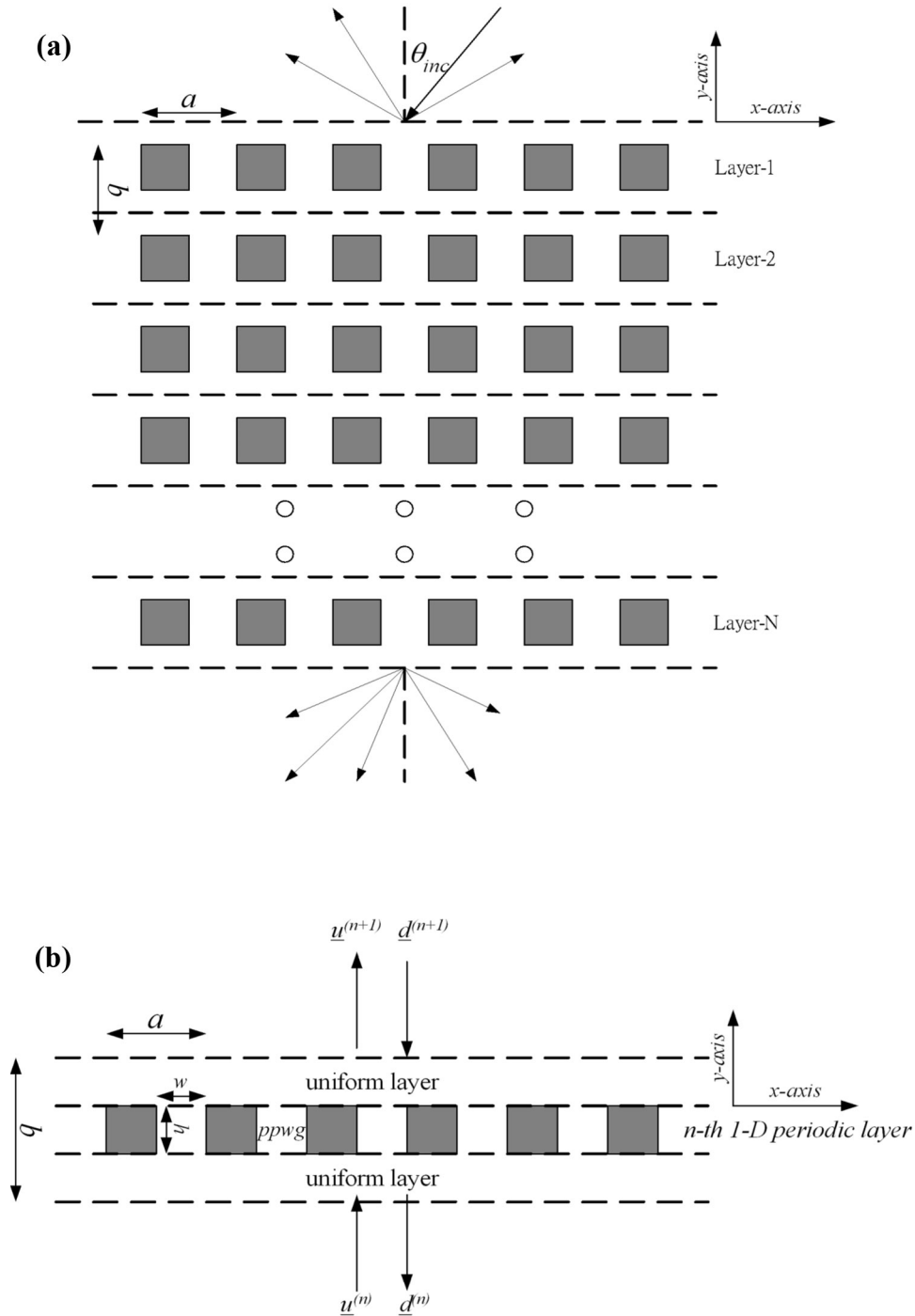

Figure 1. Structure configuration of a 2-D periodic structure made up of a stack of 1-D periodic layers: (a) 2-D periodic structure and (b) 1-D periodic layer.

metallic periodic layers, each consisting of metallic rods placed periodically along the x direction. The metal rods are taken as perfect electric conductors (PECs). We highlight the unit cell of the structure and specify its geometrical parameters, as shown in Figure 1b. The width and thickness of the metal rods are w and h, while the periods along the x and y directions are a and b, respectively. The relative dielectric constant of the host medium is ε_r. Assuming that a plane wave is obliquely incident from the air region and has no field variation along the z direction, we have a scalar boundary value problem that can always be formulated in terms of the transverse electric or transverse magnetic waves separately.

3. Method of Analysis

[11] The mathematical analysis for such type of problems was developed by many researchers; for example, the numerical method containing the finite difference method [*Maystre*, 1994], the finite difference time domain method [*Mekis et al.*, 1999], and the eigenmode method [*Noponen and Turunen*, 1994] were employed to carry out the calculation for the scattering or guiding characteristics of the photonic crystals (or 2-D periodic structures) of finite thickness. As to the analytical formulation, the Green's function based on lattice sums was employed to calculate the scattering characteristics of 2-D photonic crystals, consisting of an array of circular metallic cylinders of infinite extent [*Nicorovici and McPhedran*, 1994; *Botten et al.*, 2000]. In this paper, we utilized the rigorous mode-matching method and the Floquet solutions to formulate such a 2-D boundary value problem [*Elliott*, 1954; *Hwang*, 2004]. The outline for the analysis procedure will be illustrated in the next paragraph.

[12] Since the metal cylinder arrays are taken as PECs, the electromagnetic fields exist only in the regions between two neighboring rods and can be expanded in terms of the parallel-plate waveguide (PPWG) modes, which explicitly satisfy the boundary conditions on their surfaces. On the other hand, those in the uniform region are expanded in terms of space harmonics, each propagating as a plane wave. After imposing the continuity condition on the tangential field components across the interface between 1-D periodic and uniform layers, we can obtain an input-output relation in the form of the scattering matrix for the 1-D grating. The result so obtained for a single layer can then be cascaded for the analysis of both the scattering characteristics of the finite stack of 1-D metal gratings and the band structure of the 2-D periodic medium. For instance, the scattering characteristics of the finite stack of 1-D metal periodic layers can be determined by successively using the well-known combination rule for each scattering matrix. For the band structure calculations, one can apply the Bloch condition (periodic boundary condition) along the y direction to establish the relationship of the wave amplitudes at the two (input and output) interfaces of the unit cell to form a generalized eigenvalue problem. Each eigenvalue, in general, represents a complex propagation constant of the wave propagating in the medium, with the real and imaginary parts standing for the phase and attenuation constants along the y direction. Upon determining the eigenvalues, the corresponding eigenvector can be obtained, and thus the field profile in the structure was totally resolved. Since the detail mathematical formulation was well developed in the literature, in section 3.1, we only list some important equations for easy reference.

3.1. Scattering Matrix for a 1-D Metal Periodic Layer

[13] Referring to Figure 1b, a 1-D metal grating of finite thickness is connected to a uniform medium with the relative dielectric constant ε_r. The region between two metal rods can be regarded as a PPWG. The tangential electric and magnetic fields inside this region can be expressed in terms of the superposition of the PPWG modes, defined below:

$$\overline{E}_t(x,y) = \sum_n \overline{v}_n(y)\overline{\phi}_n(x) \tag{1a}$$

$$\overline{H}_t(x,y) = \sum_n \overline{i}_n(y)\overline{\phi}_n(x) \tag{1b}$$

$$\overline{\phi}_n(x) = \begin{cases} \sqrt{\dfrac{2}{w}}\sin\dfrac{n\pi x}{w}, & n = 1,2,3,\ldots. \\ \sqrt{\dfrac{\gamma_n}{w}}\cos\dfrac{n\pi x}{w}, & n = 0,2,3,\ldots. \end{cases} \tag{1c}$$

with $\gamma_n = \begin{cases} 1, & for\ n = 0 \\ 2, & for\ n \neq 0 \end{cases}$.

[14] In the expressions above, the functions $\overline{v}_n(y)$ and $\overline{i}_n(y)$ are the modal voltage and current of the nth PPWG mode, and they satisfy the transmission line equations

$$\frac{d\overline{v}_n(y)}{dy} = -j\overline{k}_{yn}\overline{Z}_n\overline{i}_n(y) \tag{2a}$$

$$\frac{d\overline{i}_n(y)}{dy} = -j\overline{k}_{yn}\overline{Y}_n\overline{v}_n(y) \tag{2b}$$

$$\overline{k}_{yn} = \sqrt{k_o^2\varepsilon_r - \left(\frac{n\pi}{w}\right)^2} \tag{2c}$$

$$\overline{Z}_n = 1/\overline{Y}_n = \begin{cases} \dfrac{\omega\mu_o}{\overline{k}_{yn}}; TE \\ \dfrac{\overline{k}_{yn}}{\omega\varepsilon_o\varepsilon_r}; TM \end{cases} \tag{2d}$$

where $\overline{Z}_n$ ($\overline{Y}_n$) is the characteristic impedance (admittance) of the nth waveguide mode propagating along the y direction in the PPWG region.

[15] On the other hand, the field in the uniform region (between two adjacent 1-D metal periodic layers) can be expressed as the superposition of the complete set of space harmonics, each appearing as a plane wave, given by

$$E_t(x,y) = \sum_n v_n(y)\varphi_n(x) \tag{3a}$$

$$H_t(x,y) = \sum_n i_n(y)\varphi_n(x) \tag{3b}$$

$$\varphi_n(x) = \frac{1}{\sqrt{a}} e^{-jk_{xn}x}, n = 0, \pm 1, \pm 2, \pm 3, \ldots. \tag{3c}$$

$$k_{xn} = k_x + n\frac{2\pi}{a} \tag{3d}$$

Likewise, the functions v_n (y) and i_n (y) are the modal voltage and current of the nth space harmonic, and they satisfy the transmission line equations

$$\frac{dv_n(y)}{dy} = -jk_{yn}Z_n i_n(y) \tag{4a}$$

$$\frac{di_n(y)}{dy} = -jk_{yn}Y_n v_n(y) \tag{4b}$$

$$k_{yn} = \sqrt{k_o^2\varepsilon_r - \left(k_x + n\frac{2\pi}{a}\right)^2} \tag{4c}$$

$$Z_n = 1/Y_n = \begin{cases} \dfrac{\omega\mu_o}{k_{yn}}; TE \\ \dfrac{k_{yn}}{\omega\varepsilon_o\varepsilon_r}; TM \end{cases} \tag{4d}$$

where $Z_n(Y_n)$ is the characteristic impedance (admittance) of the nth space harmonic propagating along the y direction in the uniform region.

[16] On the basis of the electromagnetic boundary conditions, the tangential electric and magnetic fields must be continuous across the step discontinuities. After matching the tangential field components at the interface by using the overlap integral between the eigenfunctions in the uniform and PPWG regions, we obtain a coupling matrix which defines the relationship between the eigenmodes in respective regions, and what follows is the scattering matrix defined at that interface. As shown in Figure 1b, we take the nth 1-D periodic layer as an example to illustrate. Since each 1-D periodic layer contains two step discontinuities and a finite length uniform transmission line in the parallel-plate region, the scattering matrix of the 1-D periodic layer is obtained by cascading these three scattering matrices, yielding

$$\begin{pmatrix} \mathbf{u}^{(n+1)} \\ \mathbf{d}^{(n)} \end{pmatrix} = \mathbf{S}^{(n)} \begin{pmatrix} \mathbf{d}^{(n+1)} \\ \mathbf{u}^{(n)} \end{pmatrix} \tag{5}$$

where scattering matrix $\mathbf{S}^{(n)}$ is a full matrix whose elements are dependent on the structure parameters as well as the incident conditions and $\mathbf{u}^{(i)}$ and $\mathbf{d}^{(i)}$ denote the upward and downward propagating waves, respectively.

3.2. Scattering Characteristics of a Finite 2-D Periodic Structure

[17] As described in section 3.1, the 2-D periodic structure is considered as the finite stack of 1-D periodic layers. Namely, if the input-output relation of the 1-D periodic layer is determined, the scattering characteristic of the 2-D periodic structure is the cascade of those 1-D ones. This is the so-called building block approach, which was commonly used in microwave engineering. This approach possesses the advantage that we can merely replace the input-output relation of the 1-D periodic layer without reformulating the whole problem when one of the 1-D periodic layer changes its structure parameters. Thus we can synthesize an arbitrary composite structure, containing various lattice patterns but with the same period along the x direction, without any difficulty.

[18] We assume that the 2-D periodic structure contains N 1-D periodic layers. The scattering matrix for each 1-D periodic layer is denoted as S_k, where the index k is running from *1* to N. The dimension of each matrix is M by M, where M is the number of truncated space harmonics (or number of parallel-plate waveguide modes). Notice that the 1-D periodic structures under consideration here may have different configurations and structural parameters, but they must have the same period in the x direction. In any case, the whole scattering matrix of a structure can be obtained by using the combination rule of scattering matrices (defined as a circled cross), which is well known in microwave engineering [*Hall et al.*, 1988]:

$$S = S_1 \otimes S_2 \otimes S_3 \ldots \otimes S_k \ldots \otimes S_N \tag{6}$$

The scattering matrix defined above relates the upward and downward propagating waves at the input surface $y = y_i$ and output surface $y = y_o$, given below:

$$\begin{pmatrix} \mathbf{u}(y_o) \\ \mathbf{d}(y_i) \end{pmatrix} = \begin{pmatrix} S_{11} & S_{12} \\ S_{21} & S_{22} \end{pmatrix} \begin{pmatrix} \mathbf{d}(y_o) \\ \mathbf{u}(y_i) \end{pmatrix} \tag{7}$$

Assuming that a plane wave is incident onto the input surface and there is no plane wave incoming from the output region, we have $\mathbf{d}(y_o) = 0$, and then the transmission and reflection responses are given by

$$\mathbf{u}(y_o) = S_{12}\mathbf{u}(y_i) \tag{8}$$

$$\mathbf{d}(y_i) = S_{22}\mathbf{u}(y_i) \tag{9}$$

where $\mathbf{u}(y_i)$ is the voltage vector of incident plane wave and $\mathbf{d}(y_i)$ and $\mathbf{u}(y_o)$ are the reflected and transmitted voltage vectors, respectively.

3.3. Dispersion Relation of Wave Propagating in the 2-D Periodic Medium

[19] In addition to the scattering characteristics for a finite thickness 2-D periodic structure, in this section, we would like to investigate the dispersion relation of the waves propagating in a 2-D periodic medium. According to Bloch's condition, a wave traveling through a period b, as shown in Figure 1b, experiences a phase difference (λ), that is,

$$\mathbf{u}^{(n+1)} = \lambda\mathbf{u}^{(n)} \tag{10a}$$

$$\mathbf{d}^{(n+1)} = \lambda\mathbf{d}^{(n)} \tag{10b}$$

By substituting (10a) and (10b) into (7), we obtain the following matrix equation:

$$\begin{pmatrix} S_{12} & O \\ S_{22} & -I \end{pmatrix} \begin{pmatrix} \mathbf{u}^{(n)} \\ \mathbf{d}^{(n)} \end{pmatrix} = \lambda \begin{pmatrix} I & -S_{11} \\ O & -S_{21} \end{pmatrix} \begin{pmatrix} \mathbf{u}^{(n)} \\ \mathbf{d}^{(n)} \end{pmatrix} \tag{11}$$

Equation (11) is a generalized eigenvalue problem with the form $A\mathbf{x} = \lambda B\mathbf{x}$, which can be solved immediately by conventional numerical packages. Such an eigenvalue problem may be cast into a system of linear homogeneous equations, and the condition for the existence of a nontrivial solution requires the vanishing in the determinant of the coefficient matrix. This yields the dispersion relation

$$\det\begin{pmatrix} S_{12} - \lambda I & \lambda S_{11} \\ S_{22} & -I + \lambda S_{21} \end{pmatrix} = 0 \tag{12}$$

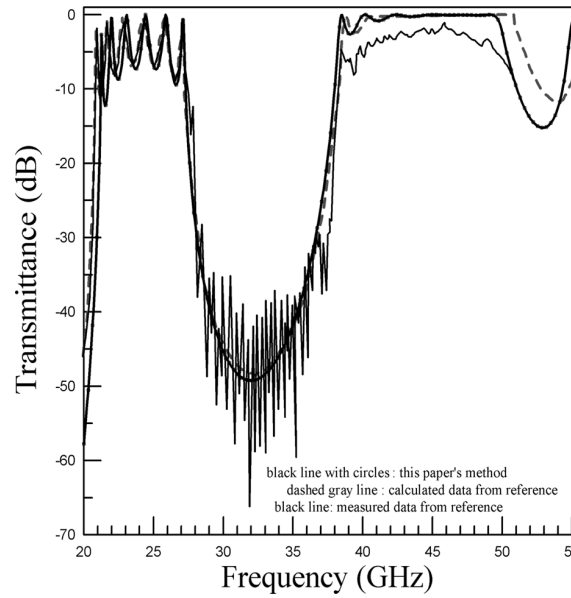

Figure 2. Comparison of the transmittance efficiency of a 2-D periodic structure containing a metal rod array among the experimental and numerical results [after *Botten et al.*, 2000] and our numerical results using the mode-matching method.

Here, the eigenvalue λ represents the phase delay of a wave traveling through a period along the y direction. It depends on the propagation constant (k_y) and the period b as well and can be written as

$$\lambda = \exp(-jk_y b) \tag{13}$$

[20] So far, we have derived the dispersion relation of the waves propagating in such a class of 2-D periodic medium. We have the relationship among the three parameters k_x, k_y, and k_o, of which any desired parameter may be determined for a given set of the other two parameters. For example, if the incident condition is specified for the component of k_x under a certain frequency of operation k_o, we can determine the value of k_y by solving the eigenvalue in (11). With k_o fixed, the relationship between k_x and k_y is referred to as the phase relation; on the other hand, with k_x fixed, the relationship between k_o and k_y is defined as the dispersion relation. In general, k_y is a complex number; its real and imaginary parts represent the phase and attenuation constants of the wave, propagating along the y direction, respectively. Similarly, we can also have the value of k_x for a given incident condition k_y by exchanging the variable x with y. Through the rigorous analysis presented so far, we have

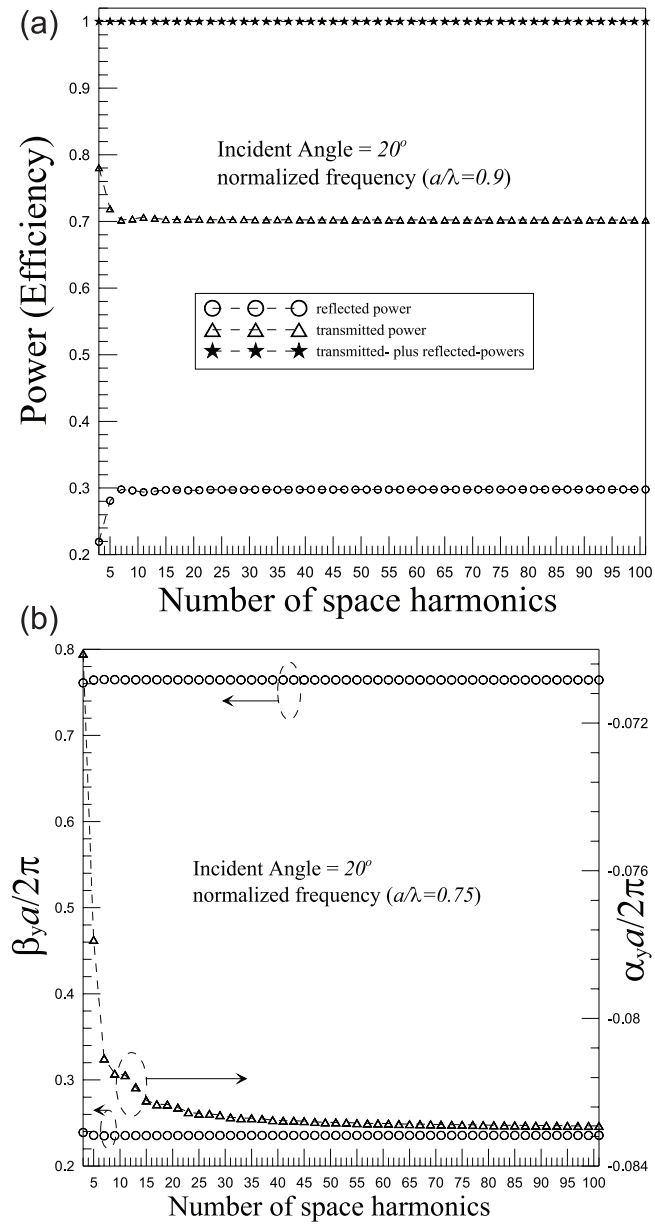

Figure 3. (a) Convergence test for the transmitted and reflected efficiencies versus number of space harmonics. (b) Convergence test for the dispersion roots of the wave propagations in a 2-D periodic medium versus number of space harmonics.

derived the phase relation as well as the dispersion relation of the waves in such a class of 2-D periodic PEC rod array. Furthermore, the field distribution can be derived from the eigenvector in (11), which defines the mode amplitudes for the upward and downward propagation waves. Moreover, from (11), we can obtain the field distribution inside the uniform transmission lines, and then the field distribution in each region can be completely determined.

4. Numerical Results and Discussion

[21] To prove the accuracy of the present method, we compared our numerical results with those (using

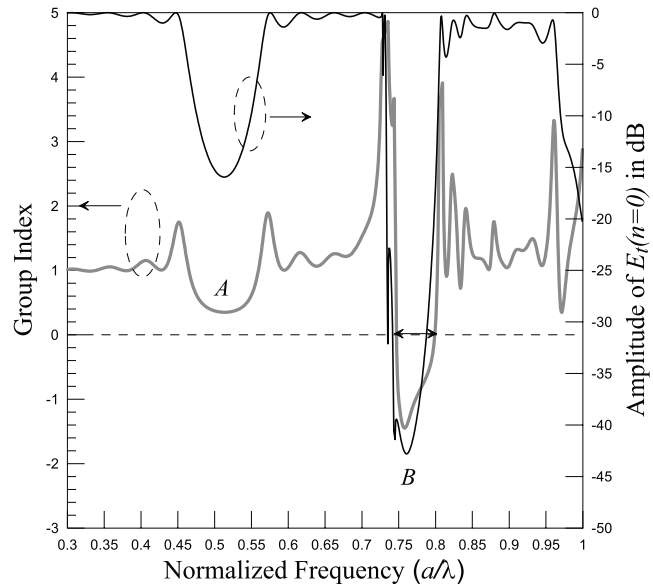

Figure 4. Variation of the transmittance and the group index for the finite 2-D periodic structure with transverse magnetic polarization and $\theta_{inc} = 20°$.

Green's function and lattice sums) in the literature [*Botten et al.*, 2000], as shown in Figure 2. The structure under consideration is a square array consisting of seven metal gratings; the array constant is 6 mm, and the radius of the circular cylinder is 0.75 mm. Since the metallic rods are in the shape of circular cylinders in that paper and our method is based on the rectangular shape of the metal rods, we take a square rod with the same area as that of the circular one, that is, $w = h = r\sqrt{\pi}$, where r is the radius of the circular cylinder. We found that the results agree well even for the ripples of the curve. Note that in the stop band regions, the results differ a little. This may be due to the edge effect of the rectangular rod in the high-frequency range, and then the stop band behavior is more significant than that of the circular one.

[22] In the following numerical examples, we calculate the scattering of plane waves by a two-dimensionally metallic cylinder arrays. Hereafter, we have normalized all the dimensions to period a along the x direction. The width of the square cylinder is assumed to be $0.25a$. The number of periods along the y direction is 10.

[23] Figure 3a depicts the convergence test for the transmitted and reflected efficiencies against the number of space harmonics employed in the numerical analysis. We changed the number of space harmonics progressively from 3 to 101 to inspect the variation of transmitted and reflected efficiencies (powers). The incident angle was assumed to be $\theta_{inc} = 20°$. The operation normalized frequency was $a/\lambda = 0.9$. In this calculation, the incident power was normalized to unity for easy checking of the power conservation criterion. The incident power must be equal to the sum of the transmitted and reflected powers (power conservation), since the metal cylinders were assumed to be lossless (perfect electric conductors). From Figure 3a, we can observe that the total power (transmitted plus reflected powers) actually is equal to unity (the error percentage is less than 10^{-6}%). Besides, both the transmitted and reflected power converge to certain values as the number of space harmonics is greater 25.

[24] Figure 3b shows the convergence test for the dispersion relation of the 2-D periodic medium against the number of space harmonics (modes in parallel-plate region) employed in the numerical calculation. The incident angle was assumed to be $\theta_{inc} = 20°$. To demonstrate the flexibility of the dispersion roots searching, the normalized frequency was designated as $a/\lambda = 0.75$, which corresponds to the complex roots in the stop band region. We changed the number of space harmonics progressively from 3 to 101 to inspect the variation of the dispersion roots ($k_y = \beta_y - j\alpha_y$). From Figure 3b, it is obvious that the dispersion roots converge to certain values as the number of space harmonics is greater than 40.

[25] Prior to demonstrating the numerical results concerning negative group velocity, we define some parameters frequently used in the ensuing numerical examples as follows. When we neglect the end effect due to the two interfaces at the input and output ports, the phase constant of the wave propagating in a 2-D periodic

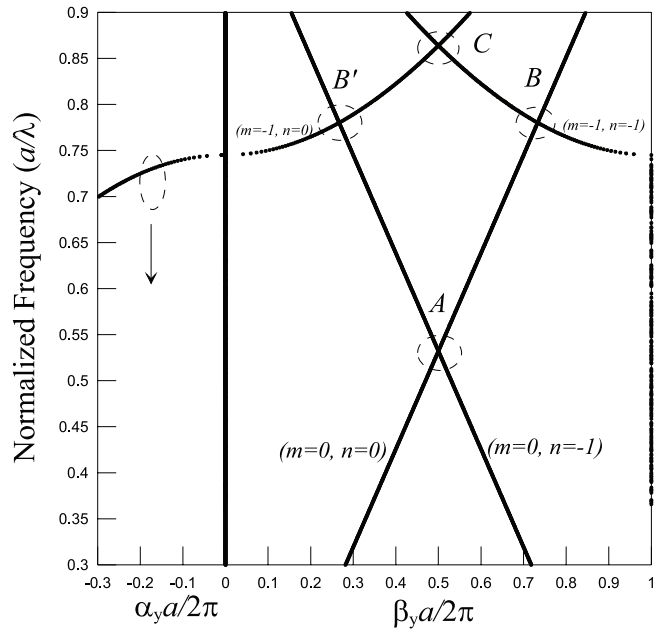

Figure 5. Unperturbed dispersion curves for the 2-D periodic medium.

structure is approximated by $\phi = -\beta L$, where ϕ is the phase angle in radians, β is the phase constant, and L is the total length where the wave propagates through. Thus the phase velocity could be written as $v_p = \omega/\beta = -L\omega/\phi$. On the other hand, the group index n_g is defined as the ratio of C to group velocity v_g, where C is the speed of light propagating in vacuum. Moreover, the relation between the group index and phase angle is written as

$$n_g = -\frac{1}{L}\frac{d\phi}{dk_o}$$

[26] Figure 4 shows the transmittance spectra of the tangential electric field component of the fundamental space harmonic $n = 0$. The amplitude and group index are shown with respect to the vertical axes in the right-hand and left-hand sides, respectively. From Figure 4, we found that there are two strong reflections, denoted by A and B, which are due to the stop bands in the two-dimensionally periodic structure. In the second stop band, apparently, there is a stronger reflection than that of the first one. Therefore we know that the second stop band has a stronger attenuation constant than the former one. It is interesting to note that the two stop bands have similar responses in amplitude distribution; nevertheless, they have distinct responses in the group index. For instance, in the first stop band region, the group index is smaller than unity, which means that the group velocity is superluminal. Besides, in the second stop band, the group index is negative, which contradicts the first one. Therefore we may conjecture that there definitely exist some unique physical insights behind the second stop band. In order to explore the basic physical mechanism for such an anomalous phenomenon, we will employ the dispersion relation of wave propagation in a two-dimensionally periodic medium to interpret the underlying physics.

[27] On the basis of the previous studies [*Hwang*, 2004], the scattering characteristics of a two-dimensionally periodic structure with finite thickness can be predicted by the dispersion relation of the same structure but with infinite extent (2-D periodic medium). Before calculating the rigorous dispersion curves of the 2-D periodic medium, we first consider a small perturbation problem; that is, the periodic variations along the x and y directions tend to zero. Under this assumption, we can have a simple equation to approximate the dispersion relation of the space harmonics in the x and y directions, which is given as

$$\left(k_x + m\frac{2\pi}{a}\right)^2 + \left(k_y + n\frac{2\pi}{a}\right)^2 \approx k_o^2 \varepsilon_{eff} \qquad (14)$$

where k_x and k_y are the propagation constants along the x and y directions, respectively. The indexes m and n, ranging from negative to positive infinity, are the space harmonics along the x and y directions. The parameter ε_{eff} is the effective dielectric constant of the medium. Figure 5 depicts the dispersion curves for the small

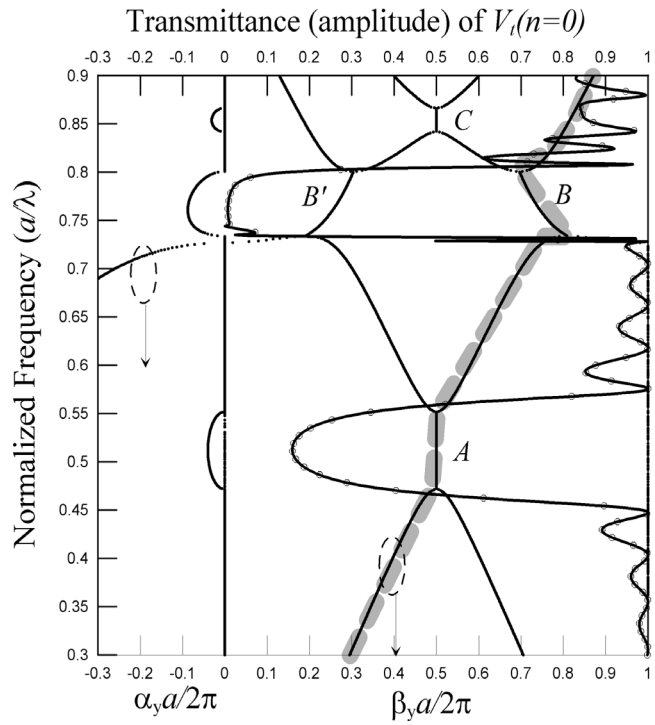

Figure 6. Exact dispersion curves for the 2-D periodic medium and the strength of transmittance for the 2-D periodic structure with finite thickness.

perturbation approximation obtained by (14). In this example, the propagation constant along the x direction is set to be $k_x = k_o \sin 20°$. The horizontal axis represents the phase (right-hand side) and attenuation (left-hand side) constants along the y direction, while the vertical axis denotes the normalized frequency a/λ. The index pair attached to each curve shows the order of space harmonic; the first one is for the x direction, and the second one is for the y direction. For example, the two straight lines denoted by ($m = 0$, $n = 0$) and ($m = 0$, $n = -1$) represent the curves contributed by the 1-D periodic structure along the y direction only, while the two hyperbolic curves denoted by ($m = -1$, $n = 0$) and ($m = -1$, $n = -1$) attribute to the periods in both the x and y directions. On the basis of coupled-mode theory, the intersection of two dispersion curves stands for the phase matching between two waves. The contraflow or coflow coupling occurs in the vicinity of intersection points. In this example, the intersection points marked by circles and arranged in alphabetical order are mainly due to the contraflow coupling between two space harmonics. Such a small perturbation analysis could provide us a basic understanding of the possible physical consequence involved in a 2-D periodic structure.

[28] Through the numerical computation, we obtained the exact dispersion relation of wave propagation in a 2-D periodic medium. The distribution for the propagation constant, including the phase (β) and attenuation (α) constants, against frequency is plotted in Figure 6. The transmittance spectra for the tangential electric field component of the fundamental space harmonic ($n = 0$) are also plotted for easy identification of the locations of stop bands. Recalling the dispersion curves and intersection points in Figure 5, one can clearly recognize the stop bands due to the contraflow coupling between space harmonics. The stop bands denoted by "A" and "C" are caused by the contraflow interaction between the space harmonics in the y direction, which are similar to those in a 1-D periodic structure. On the contrary, the stop bands denoted by "B" and "B'" are due to the combined effect of the periodicities in both the x and y directions. In addition, by tracing the transmission spectra, we know that the corresponding dispersion curve, highlighted by the heavy line, follows the fundamental space harmonic ($m = 0$, $n = 0$). Along this dispersion curve, it is interesting to note that the stop band denoted by "B" is slanted at an angle on the k_o-β diagram. In Figure 6 we compare the transmission spectrum to the dispersion curve and observe that the regions of strong reflection in the scattering of the plane do coincide with the stop bands of the wave propagation in an infinite medium, and the negative group index occurs in the slanted stop band region in which the phase

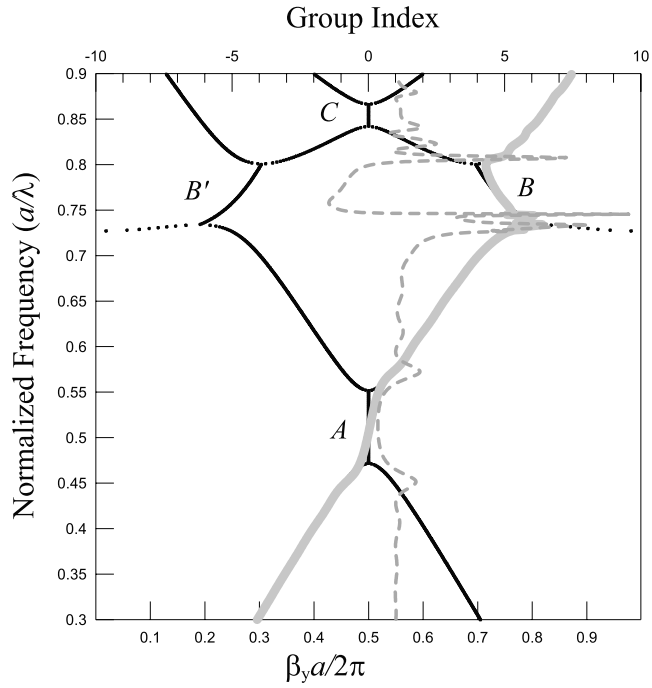

Figure 7. Distribution of the normalized phase constant versus normalized frequency. The solid black line is obtained from the exact dispersion relation, and the line with circles is obtained from the phase of transmittance spectra.

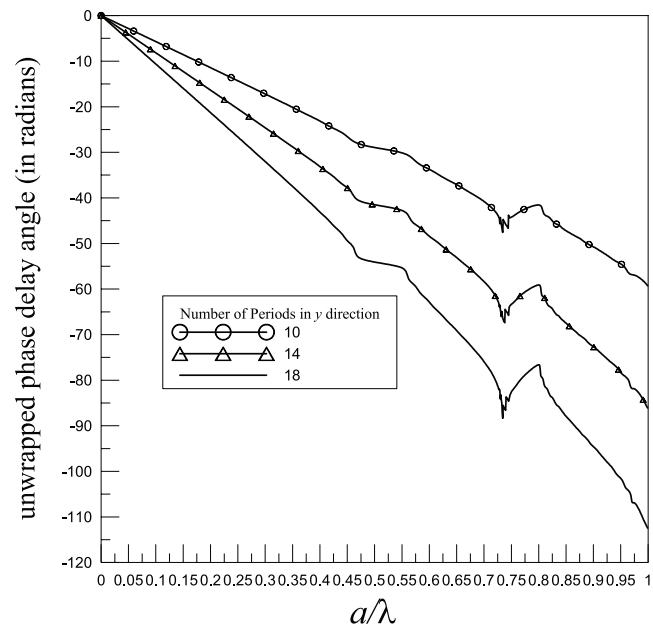

Figure 8. Unwrapped phase angle versus frequency for various thicknesses of 2-D periodic structures.

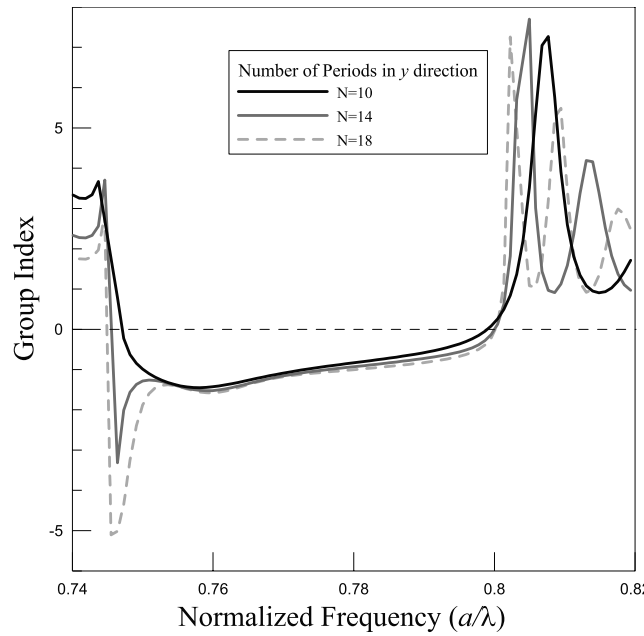

Figure 9. Distribution of group index against normalized frequency for various thicknesses for the 2-D periodic structure.

curve has a negative slope. Consequently, it is evident that in the slanted stop band region, the wave possesses a negative group velocity. In short, through the calculation on the dispersion relation of the waves propagating in a 2-D periodic medium, we prove that the negative group index is contributed by the slanted stop band, which is due to the contraflow interaction between the fundamental space harmonic and the higher-order space harmonic contributed by the combined effect in both periodicities.

[29] On the other hand, we calculated the normalized phase constant by using the phase delay angle of the transmittance spectra, which is presented in Figure 7. The real part of the dispersion roots was attached for easy reference. The normalized phase-constant curve obtained by the scattering analysis follows that obtained by the dispersion analysis of the 2-D periodic medium. In addition, the group index of the transmittance, shown by the dashed line, has also been calculated and plotted in Figure 7. One can clearly observe that the NGV indeed occurs in the slanted stop band region. At band edges, the group velocity is zero, so the group index must be infinite. Since the group index is positive outside the slanted stop band, it must undergo a zero or a pole to become negative inside. Because the negative group index does not change sign in the vicinity of the vertical stop band, it is therefore expected to be positive infinite at the band edges. On the other hand, observe that the zero group velocity occurs exactly at the band edges. Thus we have provided a verification of the negative group velocity by analysis of both the scattering and dispersion characteristics of a wave propagating in the 2-D periodic medium. This demonstrates what could occur in the case of 2-D periodic structures but not in the 1-D cases.

[30] Figure 8 depicts the variation of unwrapped phase angle versus normalized frequency for various numbers of periods along the y direction. From Figure 8, it is clear that when the thickness of the 2-D periodic structure increases, the phase delay angle (absolute value) increases accordingly. On the basis of the approximation in phase constant ($\phi = -\beta L$) as already mentioned, it is easy to recognize that the phase constant (and velocity) must be positive ($\beta \approx -\Delta\phi/\Delta L$). Returning to Figure 7, we may conclude that the wave, transmitting through the 2-D periodic structure, has positive phase and negative group velocities (anomalous dispersion) within the slanted stop band region, while it has positive phase and group velocities outside the slanted stop band region (forward wave).

[31] Figure 9 shows the distribution of the group index against the normalized frequency for three different thicknesses of the 2-D periodic structure; the numbers of 1-D periodic layers along the y direction are $N = 10$, 15, and 20. We could observe from Figure 9 that the group delay (in absolute value) increases in accordance with the increase in the thickness of the 2-D periodic structure. Furthermore, the increase in the number of 1-D

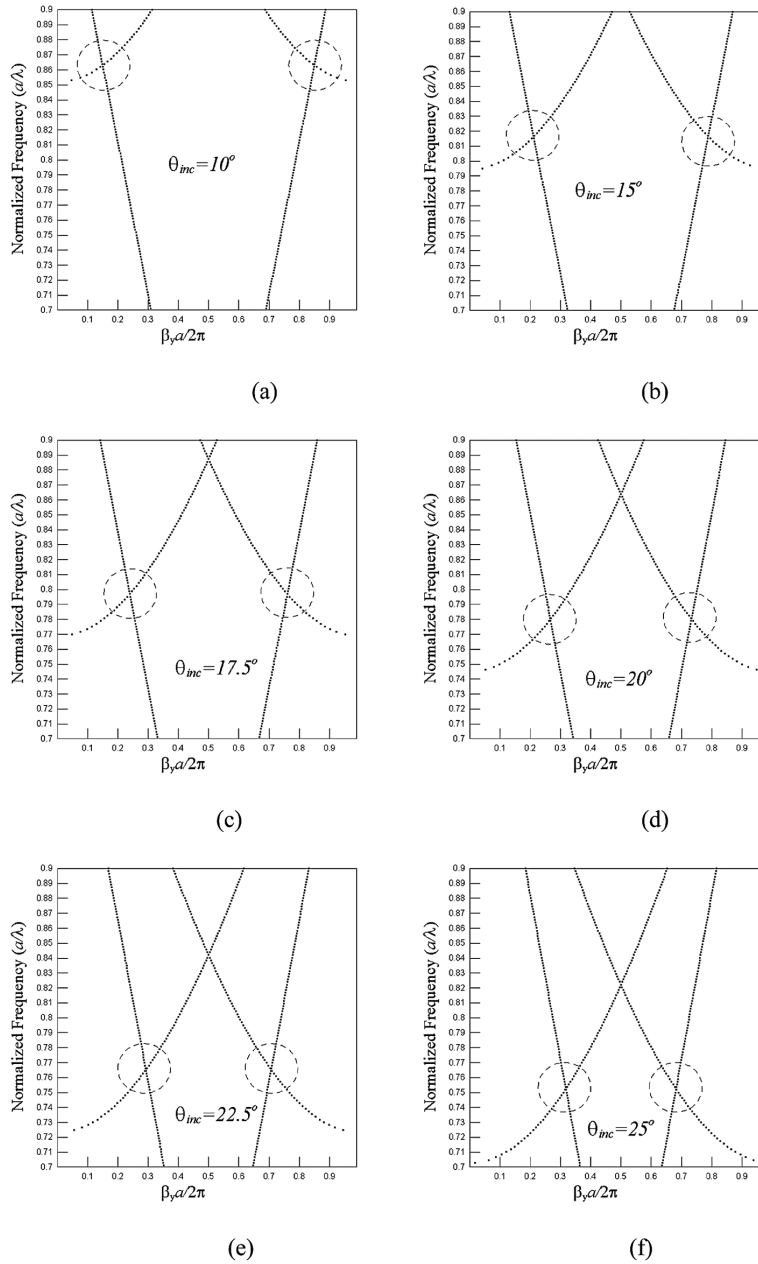

Figure 10. Unperturbed dispersion curves for a 2-D periodic structure for incident angle (a) 10°, (b) 15°, (c) 17.5°, (d) 20°, (3) 22.5°, and (f) 25°.

periodic layers only strengthens the attenuation of the wave in the stop band region. It has an insignificant effect on the bandwidth of the stop band. It is the reason why the region with negative group delay retains its bandwidth for these three cases.

[32] Since the negative group velocity occurs in the vicinity of the slanted stop band, we could expect it from the intersection of a straight line and a hyperbolic curve, as shown in the unperturbed dispersion curves in Figure 5. In Figures 10a–10f, the unperturbed dispersion curves with various incident angles were calculated to see their variations. We chose six cases (incident angle 10°, 15°, 17.5°, 20°, 22.5°, and 25°) to plot their unperturbed dispersion curves, as shown in Figures 10a–10f. From Figure 10, we may conjecture that the slanted stop band (the frequency range with negative group velocity) region

Table 1. Frequency Range of Negative Group Velocity for Various Incident Angles

Incident Angle, deg	Normalized Frequency (a/λ) Start	Normalized Frequency (a/λ) Stop
0.0	1.1930	1.3340
10.0	0.8537	0.8612
15.0	0.7943	0.8270
17.5	0.7685	0.8124
20.0	0.7473	0.7989
22.5	0.7255	0.7877
25.0	0.7043	0.7756
35.0	0.6613	0.7348
45.0	0.6411	0.6786
55.0	0.6480	0.7545
65.0	0.6509	0.7950
75.0	0.6752	0.8410
85.0	0.6996	0.8671

moves toward low normalized frequency as the incident angle increases.

[33] In addition to the case shown in Figure 4, we have also calculated some examples with different incident angles to see the variation on the frequency range of negative group velocity. For easy comparison, the frequency range of negative group velocity corresponding to each incident angle is listed in Table 1. From Table 1, we can observe that the frequency range with negative group velocity moves toward the low-frequency range as the incident angle of the plane wave increases.

5. Conclusions

[34] In this paper, we employed the mode-matching method to carry out the scattering analysis for a finite 2-D periodic structure containing a metallic cylinder array. We have found that the negative group delay occurs in the slanted stop band rather than the vertical stop band. Furthermore, the dispersion relation of waves propagating in a 2-D periodic medium was calculated by using the generalized eigenvalue method. By using the coupled-mode theory, we have established a close correlation between the NGV and the slanted stop band resulting from the combined effect of the periodicities in both the x and y directions. Since the NGV occurs in the slanted stop band region, the incident plane wave should experience a strong reflection. In order to have a practical application for the NGV property, a 2-D periodic structure may be built within a gain medium to compensate the reflection losses.

[35] **Acknowledgments.** The author would like to thank the National Science Council of the Republic of China, Taiwan, for financially supporting this research under contract NSC 94-2213-E-009-069. In addition, the author would like to thank S. T. Peng, emeritus professor at National Chiao Tung University, Hsinchu, Taiwan, for his encouragement and valuable comments in improving this manuscript. The author would like to thank the reviewers for their valuable comments in revising this manuscript.

References

Boris, G., S. Enoch, and G. Tayeb (2000), Anomalous refractive properties of photonic crystals, *J. Opt. Soc. Am. A Opt. Image Sci.*, *17*, 1012–1020.

Botten, L. C., N. A. Nicorovici, A. A. Asatryan, R. C. McPhedran, C. M. de Sterke, and P. A. Robinson (2000), Formulation for electromagnetic scattering and propagation through grating stacks of metallic and dielectric cylinders for photonic crystal calculations. Part I. Method, *J. Opt. Soc. Am. A Opt. Image Sci.*, *17*, 2165–2176.

Elek, F., and G. V. Eleftheriades (2004), Dispersion analysis of Sievenpiper's shielded structure using multi-conductor transmission-line theory, *IEEE Microwave Wireless Components Lett.*, *14*(9), 434–436.

Elliott, R. S. (1954), On the theory of corrugated plane surfaces, *IRE Trans. Antennas Propag.*, *2*, 71–81.

Enoch, S., G. Tayeb, and B. Gralak (2003), The richness of the dispersion relation of electromagnetic bandgap materials, *IEEE Trans. Antennas Propag.*, *51*(10), 2659–2666.

Fan, S., P. R. Villeneuve, and J. D. Joannopulos (1996), Large omnidirectional band gaps in metallodielectric photonic crystals, *Phys. Rev. B*, *54*, 11,245–11,251.

Gralak, B., S. Enoch, and G. Tayeb (2000), Anomalous refractive properties of photonic crystals, *J. Opt. Soc. Am. A Opt. Image Sci.*, *17*, 1012–1020.

Hall, R. C., R. Mittra, and K. M. Mitzner (1988), Analysis of multilayered periodic structures using generalized scattering matrix theory, *IEEE Trans. Antennas Propag.*, *36*(4), 511–517.

Hwang, R. B. (2004), Relations between the reflectance and band structure of 2-D metallodielectric electromagnetic crystals, *IEEE Trans. Antennas Propag.*, *52*(6), 1454–1464.

Hwang, R. B., and S. T. Peng (2003), Scattering and guiding characteristics of waveguides with two-dimensionally periodic walls of finite thickness, *Radio Sci.*, *38*(5), 1091, doi:10.1029/2002RS002847.

Maystre, D. (1994), Electromagnetic study of photonic band gaps, *Pure Appl. Opt.*, *3*, 975–993.

Mekis, A., S. Fan, and J. D. Joannopoulos (1999), Absorbing boundary conditions for FDTD simulations of photonic crystal waveguides, *IEEE Microwave Guided Wave Lett.*, *9*, 502–504.

Mojahedi, M., K. J. Malloy, G. V. Eleftheriades, J. Woodley, and R. Y. Chiao (2003), Abnormal wave propagation in passive media, *IEEE J. Selec. Topics Quantum Electron.*, *9*, 30–39.

Nicorovici, N. A., and R. C. McPhedran (1994), Lattice sums of off-axis electromagnetic scattering by gratings, *Phys. Rev. E*, *50*, 3143–3160.

Noponen, E., and J. Turunen (1994), Eigenmode method for electromagnetic synthesis of diffractive elements with three-dimensional profiles, *J. Opt. Soc. Am. A Opt. Image Sci.*, *11*, 2494–2502.

Notomi, M. (2000), Theory of light propagation in strongly modulated photonic crystals: Refraction like behavior in the vicinity of photonic band gap, *Phys. Rev. B*, *62*, 10,696–10,705.

Rotman, W. (1951), A study of single surface corrugated guides, *Proc. IRE*, *39*, 952–959.

Siddiqui, O. F., M. Mojahedi, and G. V. Eleftheriades (2003), Periodically loaded transmission line with effective negative refractive index and negative group delay, *IEEE Trans. Antennas Propag.*, *51*(10), 2619–2625.

Sigalas, M. M., C. T. Chan, K. M. Ho, and C. M. Soukoulis (1995), Metallic photonic band-gap materials, *Phys. Rev. B*, *52*, 11,744–11,751.

Solli, D. R., C. F. McCormick, R. Y. Chiao, and J. M. Hickmann (2003), Experimental observation of superluminal group velocities in bulk two-dimensional photonic bandgap crystals, *IEEE J. Selec. Topics Quantum Electron.*, *9*, 40–42.

R. B. Hwang, Department of Communication Engineering, National Chiao Tung University, 1001, Ta-Hsueh Road, Hsinchu 300, Taiwan. (raybeam@mail.nctu.edu.tw)